Desalination and Water Treatment
www.deswater.com

doi: 10.5004/dwt.2021.26672

213 (2021) 240–247
February

In-situ measurement of Auramine-O adsorption on macroporous adsorption resins at low temperature using fiber-optic sensing

Tursunjan Aydan†, Jing-Jing Yang†, Turghun Muhammad*, Fei Gao, Xiao-Xia Yang, Yi-Ting Hu

Xinjiang Key laboratory of Oil and Gas Fine Chemicals, School of Chemical Engineering and Technology, Key Laboratory of Energy Materials Chemistry, Ministry of Education, Key Laboratory of Advanced Functional Materials, Autonomous Region, Institute of Applied Chemistry, College of Chemistry, Xinjiang University, Urumqi 830046, Xinjiang, China, emails: turghunm@xju.edu.cn (T. Muhammad), nihat07@163.com (T. Aydan), yangjingjing828@sina.com (J.-J. Yang), 532212697@qq.com (F. Gao), 1531442136@qq.com (X.-X. Yang), 1589649327@qq.com (Y.-T. Hu)

Received 11 April 2020; Accepted 12 October 2020

ABSTRACT

Liquid-phase adsorption (LPA) at low temperature (e.g., 258 K) based on fiber-optic sensing was developed. Auramine-O (AO) and macroporous adsorption resins (MARs) were selected as adsorbate and adsorbent, respectively. A thermostatic adsorption vessel was designed and connected to a condensing circulating pump to enable the measurement of LPA at low temperatures. The adsorption measurement vessel contained a conical flask, a magnetic stirrer, a nylon adsorption bag, and a fiber-optic probe. Here, the adsorption bag enabled *in-situ* light absorption measurement by eliminating the interference of sorbent particles with the aid of the membrane. Adsorption conditions such as solvent, sorbent, and temperature were optimized. At a relative low-temperature range from 258 to 283 K, the adsorption capacity of HPD300 for AO increases with temperature, which was a spontaneous, endothermic adsorption process. On the contrary, at near room temperature region from 283 to 308 K, adsorption capacity decreases with temperature and it's a favorable, exothermic adsorption process. The AO adsorption process fits the Freundlich model better than the Langmuir model under the system at all temperatures. Maximum adsorption of auramine-O on HPD300 resin was obtained at 283 K. This approach could provide facile and accurate measurement of adsorption in a wide range of temperatures.

Keywords: Low temperature; Liquid-phase adsorption; Auramine-O; Fiber-optic sensing; *In-situ* measurement

1. Introduction

Liquid-phase adsorption plays a very important role in many fields. However, sampling and determination of adsorption in the liquid phase, is still being operated off-line, due to the complexity of the system comparing to the gas phase [1,2]. Gas-phase adsorption has been developed earlier and growing rapidly. Thomas et al. [3] reported the *in-situ* kinetic measurements of gas-phase firstly in 1991. An *in-situ* gas-phase thermal desorption spectroscopy was developed to investigate the adsorption/desorption of hydrogen by Pd clusters [4]. Comparatively, the measurement of liquid-phase adsorption (LPA) was complicated due to the existence of solvent. Daems et al. [5] studied the LPA of alkane/alkene mixtures on NaY zeolites using both static and flow-through adsorption methods. MacKenzie reviewed the passive solid-phase adsorption method for real-time monitoring of micro algal toxins in freshwater systems [6]. This method can be used as a supplementary technique to reduce labor-cost associated with the traditional shellfish monitoring method. Cavezza et al. [7] reported *in-situ* methanol adsorption onto aluminum oxide monitored by

* Corresponding author.

† These authors contributed equally to this work.

an integrated attenuated total reflectance Fourier-transform infrared spectroscopy system. This integrated approach is an excellent way to characterize the effect of solvent on the metal oxide surface *in-situ* at the liquid/solid interface, but the detection system is complicated.

The conventional measurements of adsorption thermodynamic in the liquid phase were generally tedious, labor-cost, and time-consuming. Adsorption temperature cannot be strictly controlled throughout the experiment due to the effect of sampling, filtration, centrifugation, or dilution processes onto the temperature. Although various analytical techniques such as liquid chromatography-mass spectrometry [8,9] and gas chromatography-mass spectrometry [10] have been applied in adsorption thermodynamics, there are still some problems to be solved. The limited data points obtained from sampling method is another weakness of traditional adsorption measurement. Thus, *in-situ*, convenient and rapid analytical techniques are needed for developing adsorption measurement in liquid phase.

Over the past 30 years, the fiber-optic sensing technology has become more popular in different scientific disciplines due to its cost-effectiveness, compactness, flexibility, and high accuracy [11]. Fiber-optic sensors possess the capability of translating a change of target analyte into optical signals and subsequently transmitting an optical signal with target analyte information to people, machines, or systems in real-time, even from a long distance [12]. Fiber-optic sensing based on ultraviolet-visible adsorption has been widely used in various fields such as environmental monitoring [13], explosive gas detection [14], drug dissolution tests [15], and on-line sampling [16,17].

Auramine (4,4-dimethylaminobenzophenonimide) and its hydrochloride salt are extensively used in the paper, textile, leather, plastic, and carpet industry [18,19]. Auramine-O (AO), a cationic basic dye, is an important organic chemical raw material and its chemical structure is shown in Fig. 1. It is soluble in water and ethanol [20]. Colored materials and dyes are non-biodegradable, highly persistent, and cause pollution. Dye manufacturers always use the cheapest and stable dyes such as AO [21]. The International Agency for Research on Cancer has proved that AO has carcinogenic ability amongst the chemicals which are associated with biotransformation of reactive species in target organs of humans and rats [22]. Therefore, it is an urgent task to remove AO from wastewater through an economical and environmentally friendly way. Among various treatment methods, adsorption is the most attractive approach due to it is simplicity, high removal efficiency, and economic feasibility [23–26].

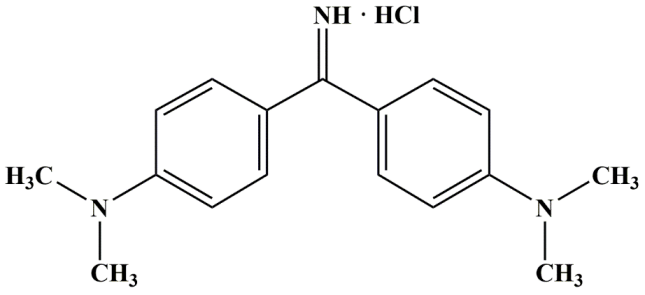

Fig. 1. Chemical structure of Auramine-O.

Herein, we report an in-situ measurement of LPA of AO on MARs at low temperatures (e.g., 258 K) based on fiber-optic sensing. A conical thermostatic vessel with inlet-outlet was constructed and ethanol was refluxed with a condensing circulating pump to produce low temperature. Packing adsorbents in an adsorption bag enabled in-situ light absorption measurement via eliminating interference of sorbent particles with the aid of membrane. The adsorption bag, magnetic stirrer, and fiber-optic probe were placed in the thermostatic adsorption vessel. MARs were chosen as the model sorbent for adsorption thermodynamics of AO, since they have strong adsorption capacity and low cost [27]. For comparison, the absorption spectra of AO in different solvents were tested by two spectrophotometers (traditional and fiber-optic), respectively. Adsorption parameters such as solvent, sorbent, and temperature were optimized. The adsorption behavior and mechanism of AO in liquid phase were discussed.

2. Experimental

2.1. Materials

Six MARs including AB-8, D101, HPD300, HPD500, HPD600, and NKA-9 were purchased from Cangzhou Bon Adsorber Technology Co., Ltd., (Hebei, China). Auramine-O was obtained from Tokyo Chemical Industry Co., Ltd., (Shanghai, China). Analytical grade methanol, ethanol, sodium hydroxide, KH_2PO_4, and K_2HPO_4 were purchased from Sinopharm Chemical Reagent (Shanghai, China) and ultrapure water was obtained from a water purification system (Chengdu, China).

2.2. Instrumentation

Fig. 2 shows the schematic diagram of the fiber-optic detection system for liquid-phase adsorption. System configurations such as light source, detector, and fiber-optic probes are the same as those reported in our previous paper [1]. A conical thermostatic vessel with inlet-outlet was designed and connected to a condenser circulating pump which produces low temperature using ethanol as a

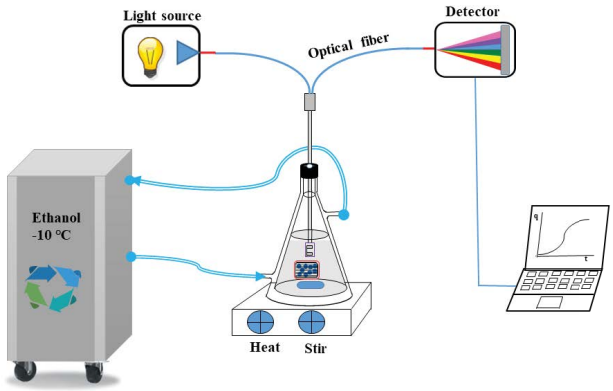

Fig. 2. Scheme of low temperature adsorption measurement system.

cooling agent. Magnetic stirrer, adsorption bag, and fiber-optic probe were placed in the thermostatic adsorption vessel for *in-situ* measurement of adsorption thermodynamics.

2.3. Activation of MARs

The activation process of MARs was described in our previous papers [1,2]. In brief, 0.1 g MARs were sealed into a 200-mesh nylon bag (2 cm × 2 cm) and put into the conical flask with a cover. Resins were immersed in ethanol for 46 h and then rinsed with water thoroughly till no residual ethanol was found. Activated MARs in bags were obtained after air-dried.

2.4. AO standard curve

A 1,000 mg L^{-1} stock solution was prepared by accurately weighing and dissolving 0.0500 g of AO in 50 mL methanol. Different volumes of AO were aspirated from the stock solution and diluted with 30% methanol-PBS (pH = 8.3), 30% methanol-water (*v*:*v* = 3:7), and 30% ethanol-water mixtures, respectively, to prepare AO with the concentration range from 0.5 to 10 mg L^{-1}. Absorbance of AO was measured using traditional and fiber-optic spectrophotometer at maximum absorption wavelength (435 nm), respectively. The calibration curves of the relationships between absorbance and concentration were obtained.

2.5. Adsorption measurement

The adsorption bag filled with activated sorbent HPD300 (0.1 g) was put into the adsorption vessel containing 150 mL of AO in 30% methanol-PBS (*v*/*v* = 3:7, pH = 8.3), with the initial concentrations (C_0) of AO ranging from 2 to 10 mg L^{-1}. The mixture solution was magnetically stirred at 350 rpm. As shown in Fig. 2, the temperature was controlled by thermostatic vessel with inlet–outlet which linked to a condensing circulating pump. Adsorption measurement of AO was conducted by fiber-optic spectrophotometer at 435 nm at temperatures ranging from 258 to 308 K. Firstly, deuterium light source was turned on for 30 min to warm up. The spectra suite software was opened; the integration and the smoothing width time were set to 17 and 5 ms, respectively. Next, an optical probe with a 5 mm light path was selected for the measurement and dipped into reference solvent of 30% methanol-PBS (*v*/*v* = 3:7, pH = 8.3). The signal intensity level was adjusted to 3,500 counts at the corresponding detection wavelength (435 nm), the reference and dark spectra were saved. If the absorption change was no more than 0.002 within 2 h (slope $\Delta A/\Delta t < 0.001$), it was decided that the adsorption reached apparent equilibrium state. The equilibrium adsorption capacity was calculated according to the calibration curve and the following equation.

$$Q_e = \left(C_0 - C_e\right) \times \frac{V}{m} \tag{1}$$

where Q_e (mg g^{-1}) is the adsorption capacity of MARs at the equilibrium, C_0 is the initial concentration of AO, C_e (mg L^{-1}) is AO concentration at the equilibrium, m (g) is the weight of the MARs, and V (L) is the volume of the adsorption solution.

For comparison, the UV-vis spectrophotometer was used to measure the adsorption capacity of AO on MARs at room temperature. For this purpose, AO solutions in the range of 1–8 mg L^{-1} in 30% methanol-PBS were prepared, and a 0.1 g MARs adsorption bag was put into the conical flasks filled with 150 mL of AO, and the mixture was magnetically stirred at 298 K for 15 h. After the adsorption, 1 mL of AO was taken, and absorbance was measured without separation. Equilibrium concentration was calculated according to the corresponding calibration curve and adsorption capacity was obtained using Eq. (1).

3. Results and discussion

3.1. Standard curves of AO with different solvents

Absorbance from the *in-situ* method and the conventional method for AO were compared, as shown in Fig. 3a. Almost the same linearity was attained using the two detectors over the concentration range of 0.5–10 mg L^{-1}, with a regression coefficient of 0.9999. Fig. 3b and Fig. S1 show the standard curves of AO in different solvents and the linear equation of AO in 30% methanol-PBS solution is $Y = 0.1070X + 0.00925$, where Y stands for the absorbance of AO and X corresponds to the concentration of AO (mg L^{-1}). It shows that the homemade fiber-optic detection system can accurately determine the adsorption of the solution.

3.2. Investigation of the solvent

To investigate the adsorption measurement in low temperature, appropriate amount of methanol or ethanol were added to the water to avoid condensation of water below 0°C. Various 1%–35% (v) methanol or ethanol–water solvents were prepared. Mobility and icing conditions of these mixtures were tested in low temperature (248 K). Adsorption capacity of MARs decreases with an increase in methanol or ethanol content, thus 30% of organic solvent was selected to reduce the freezing points of an aqueous solution.

AO solution of 4 mg L^{-1} in 30% methanol-water (*v*/*v* = 3:7), 30% ethanol–water (*v*/*v* = 3:7) and 30% methanol-PBS (*v*/*v* = 3:7, pH = 8.3) were prepared, respectively. Adsorption bag containing HPD500 was put into the home-made thermostatic adsorption vessel. The mixture was magnetically stirred at 258 K for 15 h. The absorbance of AO was measured by fiber-optic spectrophotometer at the adsorption equilibrium. The effect of the solvent was investigated. As shown in Fig. 4a. It can be seen that the highest adsorption capacity was obtained with 30% methanol-PBS as a solvent and this solvent was selected for subsequent investigation.

3.3. Screening of adsorbent

AO solution of 4 mg L^{-1} in 30% methanol-PBS (*v*/*v* = 3:7, pH = 8.4) was prepared. Adsorption bags containing different kinds of MARs were put into the conical flasks filled with 150 mL of AO solution and mixtures were magnetically stirred at 298 K for 15 h. The absorbance of AO was measured by a traditional spectrophotometer at the adsorption

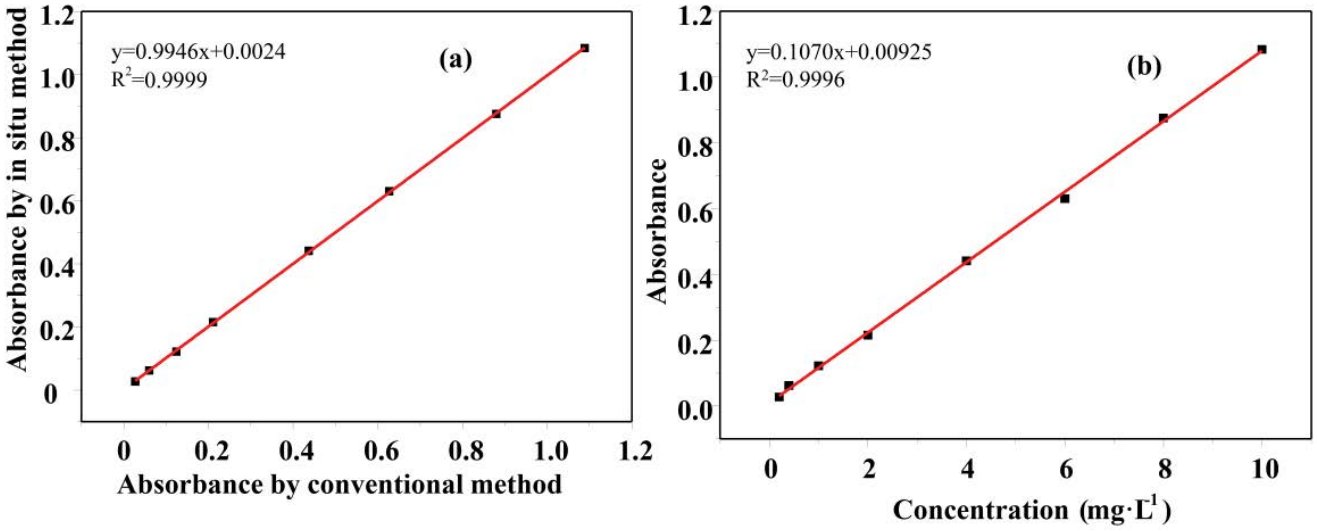

Fig. 3. (a) Comparison of absorbance from the *in-situ* method and the conventional method for AO the range of 0.5–10 mg L^{-1} and (b) standard curves of AO in 30% methanol-PBS, λ = 435 nm.

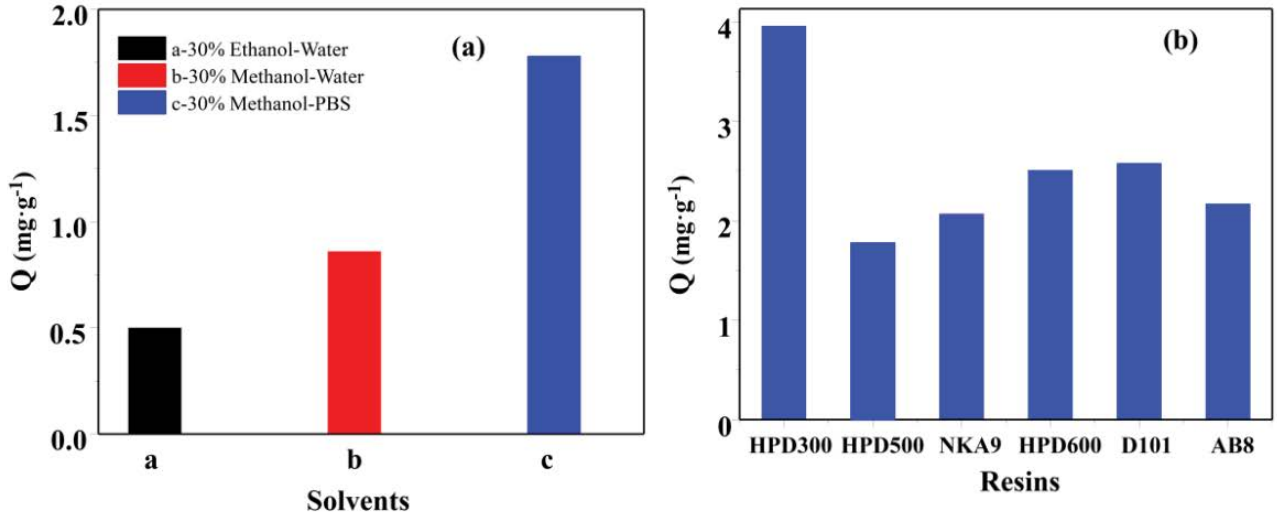

Fig. 4. (a) AO adsorption in different solvents, V = 150 mL, T = 258 K, $C_{(AO)}$ = 4 mg L^{-1}, $m_{(HPD500)}$ = 0.1 g and (b) the screening of MARs, $m_{(MARs)}$ = 0.1 g, V = 150 mL, and 4 mg L^{-1} of AO with 30% methanol-PBS (v/v = 3:7, pH = 8.4), T = 298 K.

equilibrium. The results are shown in Fig. 4b. The adsorption capacity (Q) of AO on HPD300 is the highest in these resins. The possible reason was that the polarity of HPD300 was well-matched with AO, the pore volume, and specific surface area was larger than that of others, resulting in the highest adsorption capacity. Thus, HPD300 was selected for the next investigation.

3.4. Effect of temperature

AO solutions of a series concentration in 30% methanol-PBS were prepared and adsorbed by HPD300 at various temperatures. The absorbencies of AO were measured by fiber-optic spectrophotometer at adsorption equilibrium. The results are shown in Fig. 5, in the low-temperature range (258–283 K), the adsorption capacity of AO decreases in the beginning and then increases. The adsorption capacity is the minimum at 268 K. In the high-temperature range (283–308 K), the adsorption capacity of AO decreases with temperature and reaches the maximum at 283 K, which may be due to the increase in viscosity of AO solution and the limitation of molecular movement at low temperature [28], which hinders mass transfer and reduces sorption of AO molecules to the resin, resulting in low adsorption. On the contrary, in near room temperature zone, the adsorption decreases with temperature, which indicates that the adsorption of AO on HPD300 is an exothermic process, low temperature is more favorable for this process. This result agrees well with other adsorbates [2].

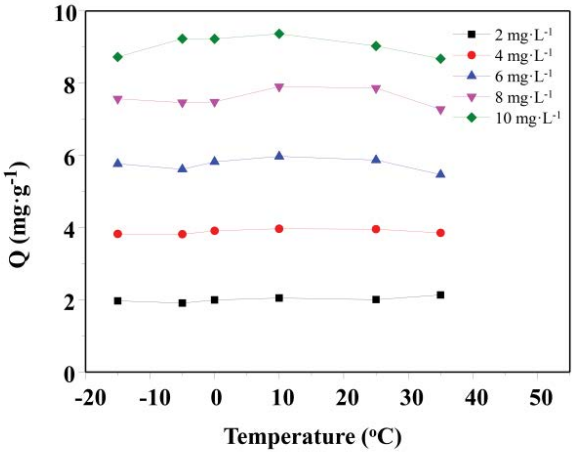

Fig. 5. Adsorption capacity of HPD300 for AO (2–10 mg L^{-1}) at different temperatures V = 150 mL, $m_{(HPD300)}$ = 0.1 g, solvent: 30% methanol-PBS (v/v = 3:7, pH = 8.4).

3.5. Adsorption thermodynamics

3.5.1. Adsorption isotherm

Adsorption isotherm is a specific description of adsorption equilibrium, which refers to the distribution of analyte in two phases at a certain temperature when adsorption reaches the equilibrium [29]. In the thermodynamic measurement, the adsorption capacity is determined as a function of temperature. Hence, it is necessary to control the temperature precisely. In this work, the Langmuir and Freundlich models were used to simulate the experimental results and adsorption process. These models may show the types of the interaction force between AO and the resin. Langmuir model [30] assumes a single layer adsorption state, which supposes that the activity of every adsorption site on the surface of sorbent is equal and the sorbate is adsorbed homogeneously without interaction. Freundlich model [31] describes a multilayer adsorption, which assumes that the surface of the sorbent is heterogeneous. Linear forms of Langmuir isotherms are expressed by the following equations:

$$\frac{1}{Q_e}=\frac{1}{Q_{\max}}+\frac{1}{Q_{\max}K_LC_e} \tag{2}$$

$$\ln Q_e=\ln K_F+\frac{1}{n}\ln C_e \tag{3}$$

In Eqs. (2) and (3), Q_e and $Q_{\max}$ (mg g^{-1}) are the relative adsorption capacity and the monolayer adsorption capacity, respectively. C_e (mg L^{-1}) is the concentration of AO at the adsorption equilibrium; K_L (L mg^{-1}) and K_F (mg g^{-1}) (L $mg^{-1})^{1/n}$ are the parameters of Langmuir and Freundlich, respectively.

The isotherm models are shown in Fig. 6, the parameters of $Q_{\max}$, K_L, K_F, and n, linear regression equation and R^2 values are shown in Table 1. By comparing of R^2, the adsorption pattern better fits Freundlich model than Langmuir model at all temperatures. It is suggested that the adsorption of AO by HPD300 is the multilayer adsorption onto a heterogeneous surface. The value of $1/n$ indicates the energy or intensity of the interaction and suggests the favorability and capacity of the sorbent-sorbate system, that is, irreversible ($1/n$ = 0), favorable ($0 < 1/n < 1$), or unfavorable ($1/n > 1$). As shown in Table 1, n is greater than 2, revealing that the AO molecule can be favorably adsorbed by HPD300 resin.

3.5.2. Thermodynamic parameters

The adsorption free energy (ΔG, kJ mol^{-1}), enthalpy (ΔH, kJ mol^{-1}), and entropy (ΔS, J mol^{-1} K^{-1}) were calculated from the adsorption of AO over HPD300 at various temperatures. Based on the thermodynamic theory, the relationship can be described by the following Eqs. (4) and (5), respectively [32,33]:

$$\ln K_L=\frac{\Delta S}{R}-\frac{\Delta H}{RT}=\frac{Q_e}{C_e} \tag{4}$$

$$\Delta G=\Delta H-T\Delta S \tag{5}$$

where R is the gas constant (8.314 J mol^{-1} K^{-1}) and T is the absolute temperature (K). ΔH and ΔS values were calculated from the slope and intercept of the linear regression of $\ln K_L$ against $1/T$, respectively. Thermodynamic parameters of AO onto the HPD300 at temperatures ranging from 268 to 283 K are listed in Table 2. The positive value of ΔH suggests the adsorption process is endothermic and an increase in temperature is beneficial to the adsorption. The positive value of ΔS indicated the

Table 1
Langmuir and Freundlich isotherm parameters for adsorption of AO on HPD300 resin at different temperatures

	Langmuir				Freundlich			
T (K)	Regression equation	$Q_{\max}$ (mg g^{-1})	K_L (L mg^{-1})	R^2	Regression equation	K_F (mg g^{-1})(L $mg^{-1})^{1/n}$	n	R^2
258	$Y = 0.00945X + 0.142$	7.042	15.03	0.8725	$Y = 0.395X + 0.922$	8.356	1.069	0.9804
268	$Y = 0.0151X + 0.128$	7.813	8.477	0.9440	$Y = 0.498X + 0.973$	9.397	2.008	0.9803
273	$Y = 0.01X + 0.138$	7.246	13.81	0.9149	$Y = 0.495X + 1.089$	12.27	2.020	0.9837
283	$Y = 0.0016X + 0.155$	6.452	96.88	0.8725	$Y = 0.291X + 0.965$	9.226	3.436	0.9877
298	$Y = 0.003X + 0.151$	6.623	50.33	0.8841	$Y = 0.343X + 0.959$	9.099	2.915	0.9658
308	$Y = 0.0043X + 0.164$	6.105	38.09	0.8791	$Y = 0.3068X + 0.864$	7.316	3.259	0.9365

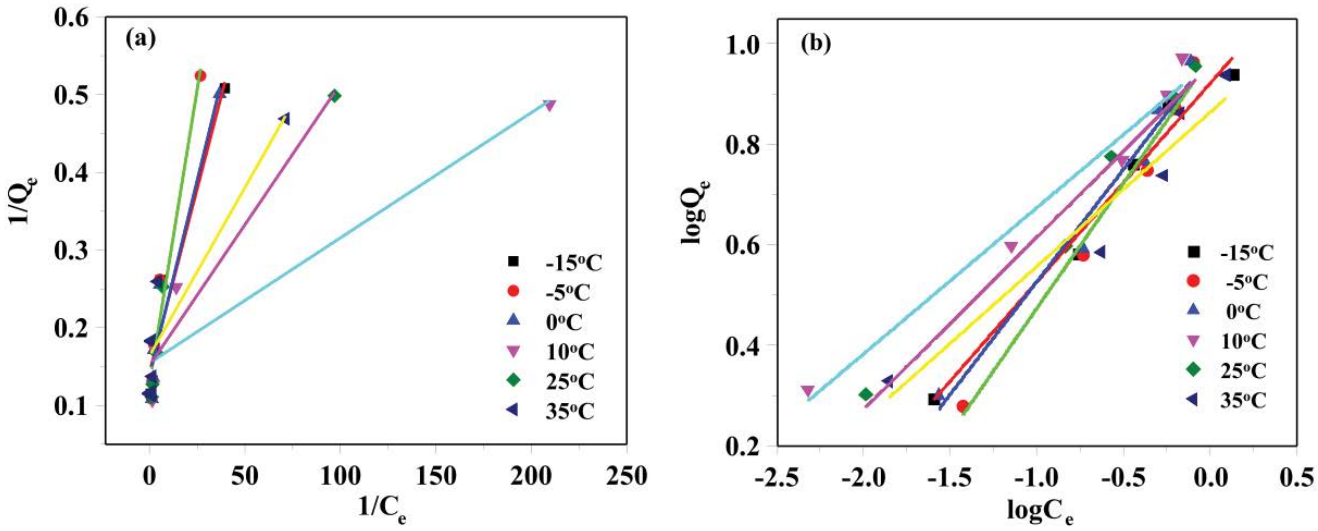

Fig. 6. Isotherm models of AO on HPD300 (a) Langmuir and (b) Freundlich.

Table 2
Parameters of the thermodynamic adsorption of AO on HPD300 at low temperature

C_0 (mg L^{-1})	ΔH (kJ mol^{-1})	ΔS (J K^{-1} mol^{-1})	ΔG (kJ mol^{-1})		
			268 K	273 K	283 K
2	92.72	0.377	–8.411	–10.09	–14.07
4	44.14	0.189	–6.461	–7.405	–9.293
6	16.07	0.0811	–5.670	–6.076	–6.886
8	5.85	0.0429	–5.640	–5.855	–6.284
10	6.98	0.0463	–5.431	–5.663	–6.126

adsorption is an entropic increase process and is associated with an increase in randomness of the solid–liquid interface. The free energy (ΔG) value of the adsorption was negative at all temperatures, which indicates that the adsorption process was spontaneous. The increase in absolute value of ΔG with temperature indicates that the higher temperature favors endothermic adsorption process of AO. This could also be evidenced by increase in binding capacity from 268 to 283 K, implying the adsorption process is result of in chemical interaction as well as of physical interaction.

In the temperature range from 283 to 308 K, thermodynamic parameters of AO on HPD300 are shown in Table 3. The negative enthalpy change (ΔH) suggests that the adsorption in this temperature range is an exothermic process, which is in accord with the decrease in adsorption capacity with temperature. The absolute values of ΔH are within 7–35 kJ mol^{-1}, indicating that physical adsorption is the main contribution of the process. The negative values of entropy (ΔS) suggest that randomness at the solid–liquid interface decreased during the adsorption of AO on HPD300 surface. It also shows that the enthalpy change is the main contribution of AO adsorption on HPD300. The negative ΔG indicates that the adsorption of AO on HPD300 is a spontaneous process. The absolute value of ΔG decreases with temperature from 283 to 308 K, indicates that the higher temperature is not favorable for exothermic adsorption process of AO.

It is obvious that very low and high temperature is not favorable for the adsorption of AO. The turning point of AO adsorption on HPD300 is 283 K, which may explain why some scholars often choose 283 K as the lowest temperature for adsorption study. However, the specific adsorption behavior and the mechanism at low temperatures need to be further studied.

4. Conclusions

A thermostatic adsorption vessel was designed and connected to a condensing circulating pump to enable the measurement of LPA at low temperatures. By comparison, the fiber-optic spectrophotometer was found to produce a calibration curve as good as a traditional spectrophotometer does and be applied in LPA. The adsorption conditions such as resin type, solvent, and temperature were optimized. HPD300 and 30% methanol-PBS (3:7, pH = 8.3) were selected as the best MARs and solvent, respectively. At a relative low-temperature range from 258 to 283 K, the adsorption capacity of HPD300 increases with temperature and it is a favorable, spontaneous, endothermic adsorption process. On the contrary, the temperature ranged from 283

Table 3
Thermodynamic parameters of AO adsorption on HPD300 at near room temperature

C_0 (mg L^{-1})	ΔH (kJ mol^{-1})	ΔS (J K^{-1} mol^{-1})	ΔG (kJ mol^{-1})		
			283 K	298 K	308 K
2	–30.81	–0.0587	–14.18	–13.30	–12.71
4	–35.33	–0.0913	–9.485	–8.114	–7.201
6	–18.63	–0.0417	–6.824	–6.198	–5.781
8	–7.501	–0.0044	–6.288	–6.202	–6.159
10	–18.17	–0.0421	–6.253	–5.622	–5.201

to 303 K, the adsorption capacity decreases with temperature and it is a favorable, spontaneous, and exothermic process. Maximum adsorption was obtained at 283 K. AO adsorption process fits the Freundlich model better than the Langmuir model at all temperatures.

Acknowledgments

This work was supported by the National Natural Science Foundation of China (22064015, 21565025); and the Natural Science Foundation of Xinjiang University (61367). The authors declare that they have no conflict of interest.

References

[1] F. Gao, T. Muhammad, M. Bakri, P. Pataer, L.X. Chen, *In-situ* liquid-phase-adsorption measurement system based on fiber-optic sensing with the aid of membranes, ACS Omega, 3 (2018) 10891–10897.
[2] F. Gao, T. Muhammad, M. Bakri, W.W. Yang, P. Pataer, X.X. Yang, *In-situ* measurement of the adsorption thermodynamics of rutin on macroporous adsorption resins by fiber-optic sensing, Instrum. Sci. Technol., 47 (2019) 170–184.
[3] R.C. Thomas, L. Sun, R.M. Crooks, A.J. Ricco, Real-time measurements of the gas-phase adsorption of *n*-alkylthiol mono- and multilayers on gold, Langmuir, 7 (1991) 620–622.
[4] M. Takenouchi, S. Kudoh, K. Miyajima, F. Mafuné, Adsorption and desorption of hydrogen by gas-phase palladium clusters revealed by *in-situ* thermal desorption spectroscopy, J. Phys. Chem. A, 119 (2015) 6766–6772.
[5] I. Daems, P. Leflaive, A. Méthivier, J.F.M. Denayer, G.V. Baron, Evaluation of experimental methods for the study of liquid-phase adsorption of alkane/alkene mixtures on y zeolites, Adsorption, 11 (2005) 189–194.
[6] L.A. MacKenzie, *In-situ* passive solid-phase adsorption of micro-algal biotoxins as a monitoring tool, Curr. Opin. Biotechnol., 21 (2010) 326–331.
[7] F. Cavezza, S. Pletincx, R.I. Revilla, J. Weaytens, M. Boehm, H. Terryn, T. Hauffman, Probing the metal oxide/polymer molecular hybrid interfaces with nanoscale resolution using AFM-IR, J. Phys. Chem. C, 123 (2019) 26178–26184.
[8] Y. Bao, F. Yuan, X. Zhao, Q. Liu, Y. Gao, Equilibrium and kinetic studies on the adsorption debittering process of ponkan (*Citrus reticulata* blanco) juice using macroporous resins, Food Bioprod. Process., 94 (2015) 199–207.
[9] C. Delitala, E. Cadoni, D. Delpiano, D. Meloni, M.D. Alba, A.I. Becerro, I. Ferino, Liquid-phase thiophene adsorption on MCM-22 zeolites. Acidity, adsorption behaviour and nature of the adsorbed products, Microporous Mesoporous Mater., 118 (2009) 11–20.
[10] S. Melchers, Y. Alsalka, J. Schneider, D.W. Bahnemann, Studies on the adsorption and photocatalytic degradation of an EuIII(TTFA)3(MePhTerpy) complex on the TiO_2 surface, J. Photochem. Photobiol., A, 364 (2018) 303–308.
[11] X.D. Wang, O.S. Wolfbeis, Fiber-optic chemical sensors and biosensors (2015–2019), Anal. Chem., 92 (2020) 397–430.
[12] X.D. Wang, O.S. Wolfbeis, Fiber-optic chemical sensors and biosensors (2013–2015), Anal. Chem., 88 (2016) 203–227.
[13] L. Ferrer, G. De Armas, M. Miró, J.M. Estela, V. Cerdà, A multisyringe flow injection method for the automated determination of sulfide in waters using a miniaturised optical fiber spectrophotometer, Talanta, 64 (2004) 1119–1126.
[14] X. Li, Q. Li, H. Zhou, H. Hao, T. Wang, S. Zhao, Y. Lu, G. Huang, Rapid, on-site identification of explosives in nanoliter droplets using a UV reflected fiber optic sensor, Anal. Chim. Acta, 751 (2012) 112–118.
[15] T. Muhammad, J. De Wang, M. Li-Wan, J. Chen, Monitoring dissolution rate of amiodarone tablets by a multiple fiber-optic sensor system, Dissolution Technol., 15 (2008) 22–27.
[16] T. Muhammad, O. Yimit, Y. Turahun, K. Muhammad, Y. Uludağ, Z. Zhao, On-line determination of 4-nitrophenol by combining molecularly imprinted solid-phase extraction and fiber-optic spectrophotometry, J. Sep. Sci., 37 (2014) 1873–1879.
[17] M. Qadir, T. Muhammad, M. Bakri, F. Gao, Determination of total polyphenols in tea by a flow injection-fiber optic spectrophotometric system, Instrum. Sci. Technol., 46 (2018) 185–193.
[18] I.D. Mall, V.C. Srivastava, N.K. Agarwal, Adsorptive removal of auramine-O: kinetic and equilibrium study, J. Hazard. Mater., 143 (2007) 386–395.
[19] C. Qi, M. Meng, Q. Liu, C. Kang, S. Huang, Z. Zhou, C. Chen, Adsorption kinetics and thermodynamics of auramine-O on sugarcane leaf-based activated carbon, J. Dispersion Sci. Technol., 36 (2015) 1257–1263.
[20] G. Zhang, L. Yi, H. Deng, P. Sun, Dyes adsorption using a synthetic carboxymethyl cellulose-acrylic acid adsorbent, J. Environ. Sci., 26 (2014) 1203–1211.
[21] M. Oplatowska-Stachowiak, C.T. Elliott, Food colors: existing and emerging food safety concerns, Crit. Rev. Food Sci. Nutr., 57 (2017) 524–548.
[22] A. Asfaram, M. Ghaedi, S. Hajati, M. Rezaeinejad, A. Goudarzi, M.K. Purkait, Rapid removal of auramine-O and methylene blue by ZnS:Cu nanoparticles loaded on activated carbon: a response surface methodology approach, J. Taiwan Inst. Chem. Eng., 53 (2015) 80–91.
[23] S.A. Hosseinpour, G. Karimipour, M. Ghaedi, K. Dashtian, Use of metal composite MOF-5-Ag_2O-NPs as an adsorbent for the removal of auramine O dye under ultrasound energy conditions, Appl. Organomet. Chem., 32 (2018) 1–11.
[24] J. Goscianska, M. Marciniak, R. Pietrzak, The effect of surface modification of mesoporous carbons on auramine-O dye removal from water, Adsorption, 22 (2016) 531–540.
[25] W. Yang, T. Muhammad, A. Yigaimu, K. Muhammad, L. Chen, Preparation of stoichiometric molecularly imprinted polymer coatings on magnetic particles for the selective extraction of auramine O from water, J. Sep. Sci., 41 (2018) 4185–4193.
[26] B.S. Inbaraj, J.T. Chien, G.H. Ho, J. Yang, B.H. Chen, Equilibrium and kinetic studies on sorption of basic dyes by a natural biopolymer poly(γ-glutamic acid), Biochem. Eng. J., 31 (2006) 204–215.
[27] Z.B. Chen, A.J. Zhang, J. Li, F. Dong, D.L. Di, Y.Z. Wu, Study on the adsorption feature of rutin aqueous solution on

macroporous adsorption resins, J. Phys. Chem. B, 114 (2010) 4841–4853.
[28] T.W. Yergovich, G.W. Swift, F. Kurata, Density and viscosity of aqueous solutions of methanol and acetone from the freezing point to 10°C, J. Chem. Eng. Data, 16 (1971) 222–226.
[29] W. Xing, H.H. Ngo, S.H. Kim, W.S. Guo, P. Hagare, Adsorption and bioadsorption of granular activated carbon (GAC) for dissolved organic carbon (DOC) removal in wastewater, Bioresour. Technol., 99 (2008) 8674–8678.
[30] L. Ding, X. Lu, H. Deng, X. Zhang, Aqueous solutions using MIEX resin, Ind. Eng. Chem. Res., 51 (2012) 11226–11235.
[31] S. Vasiliu, I. Bunia, S. Racovita, V. Neagu, Adsorption of cefotaxime sodium salt on polymer coated ion exchange resin microparticles: kinetics, equilibrium and thermodynamic studies, Carbohydr. Polym., 85 (2011) 376–387.
[32] B. Belhamdi, Z. Merzougui, M. Trari, A. Addoun, A kinetic, equilibrium and thermodynamic study of L-phenylalanine adsorption using activated carbon based on agricultural waste (date stones), J. Appl. Res. Technol., 14 (2016) 354–366.
[33] M.I. Konggidinata, B. Chao, Q. Lian, R. Subramaniam, M. Zappi, D.D. Gang, Equilibrium, kinetic and thermodynamic studies for adsorption of BTEX onto ordered mesoporous carbon (OMC), J. Hazard. Mater., 336 (2017) 249–259.

Supplementary information

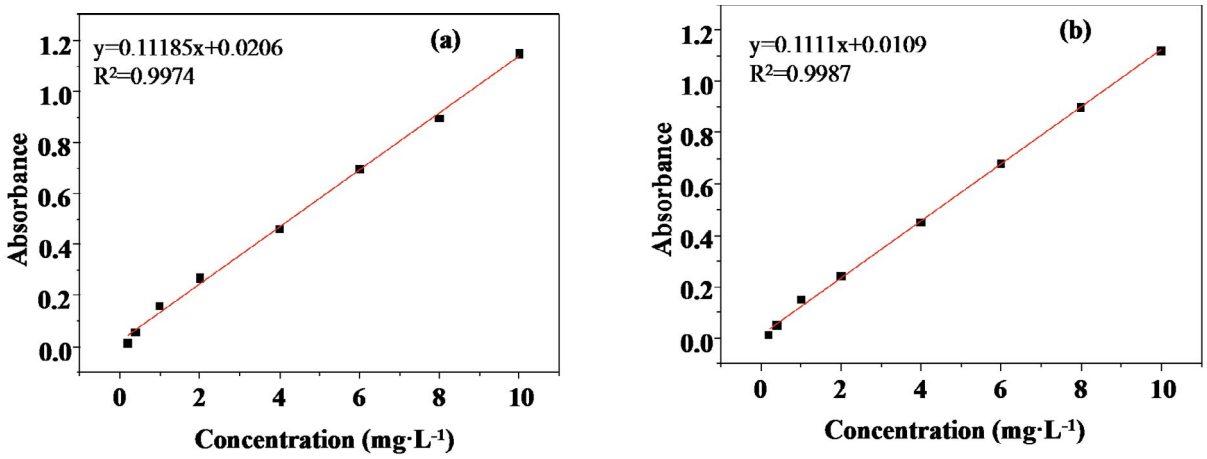

Fig. S1. Standard curves of Auramine-O in (a) 30% methanol–water and (b) 30% ethanol–water λ = 435 nm.